Numerical Investigation of Propeller-Airfoil Interaction Noise Based on Large-Eddy Simulation and FW-H method

Zhe Yang[1], Matthias Meinke, Wolfgang Schröder

Institute of Aerodynamics, RWTH Aachen University
Wüllnerstr. 5a, 52062 Aachen, Germany

Keywords:

Distributed Propulsion, Propeller-Airfoil Interaction, Propeller Noise, Large-Eddy Simulations

Introduction

Distributed propulsion systems [1] are one of the promising approaches that could achieve less emission, higher efficiency, and maneuverability for future Urban Air Mobility (UAM) aircraft. The tight integration of the propulsion system with the airframe increases the airfoil lift-to-drag ratio as well as the propeller propulsive efficiency. However, along with the aerodynamic benefits, the configuration also brings challenges to the acoustic design. On the positive side, installing the propulsion system closer to the airframe should provide interesting acoustic shielding effects [2], reducing the far-field noise level of the aircraft in certain directions. On the adverse side, the integrated design may reinforce acoustic sources due to the unsteady loads caused by potential distortion or wake/boundary layer viscous effects, increasing the overall noise emission. Some research efforts have been made to seek a balance between the aero-dynamic benefits and the noise generation [3,4].

Numerical Methods

The object of this work is to perform an analysis of the noise generation mechanisms of propeller-airfoil interactions. Large eddy simulations (LES) of a distributed propulsion system are conducted using the Multiphysics flow solver m-AIA [5] of RWTH. The unstructured hierarchical Cartesian mesh is generated according to predefined mesh parameters for the target geometry. The Navier-Stokes equations are solved by a finite volume (FV) solver at second-order accuracy in time and space to perform wall-resolved LES of the turbulent flow field. To track the rotating geometry of the propeller blades, a level-set solver based on the kinematic motion level-set approach is employed, providing information about the surface location for solution adaptive mesh refinement (AMR) during the simulation run. A postprocessing module is integrated into the simulation workflow to conduct time averaging or time-series data sampling. For the far-field noise, the Ffowcs-Williams and Hawkings (FW-H) method formulated in the frequency domain is used to predict the pressure signals at far-field observer positions. During the simulation run, dynamic load balancing (DLB) is performed to alleviate the load imbalances from the AMR and to achieve sufficient parallel computing efficiency on the high-performance computing system HAWK installed at HLRS of the University of Stuttgart.

The test geometry is the ENODISE-B1 configuration provided by TUDelft [6]. It has a tractor setup with three XPROP-S propellers which are installed upstream of a wing with an airfoil shape of NLFMod22(B). The incoming flow velocity is 30 m/s and the propeller advance ratio is 0.8. The propeller has an installation shaft incidence angle of -5 deg and the incoming flow has a +2 deg angle of attack (AoA) with respect to the wing chord. To reduce the computational cost, the simulation domain only includes the middle propeller. Periodic boundary conditions are used to mimic the effects of the two neighboring propellers. The Reynolds number based on the airfoil chord length is set to approximately 600,000 in accordance with the experimental setup. To resolve the turbulent boundary layer near the solid surfaces, the minimum spatial step near solid boundaries is chosen to be $7*10^{-5}$ m, resulting in about 200 cells along the propeller chord length and 4,000 cells along the wing chord length. Adaptive mesh refinement is applied to the fluid-solid interface with the minimum spatial resolution and coarsening to the far field until a maximum spatial step of $2*10^{-3}$ m is reached. Overall, this leads to $O(10^9)$ grid cells. The rotating propeller and the high-frequency turbulent scales are resolved with a timestep of $1*10^{-7}$ s, which is determined by the stability limit of the numerical method.

[1] z.yang@aia.rwth-aachen.de

Results and Discussion

The analysis of this work focuses on the interaction of the propeller slipstream with the downstream wing and its impact on noise generation. Aerodynamic results are shown in Figure 1, where contours of the the Q-Criterion to visualize the propeller wake and tip vortex structures are shown on the left. The tip vortices impinge on the leading edge of the wing and break down while traveling around the wing. Time series of pressure and velocity around the wing surfaces are recorded to investigate the wing turbulent flow field and to further identify potential noise sources. Fig 1 (b) shows the simulation results of the total pressure coefficient in the wake downstream of the propeller to be in good agreement with the measurement data.

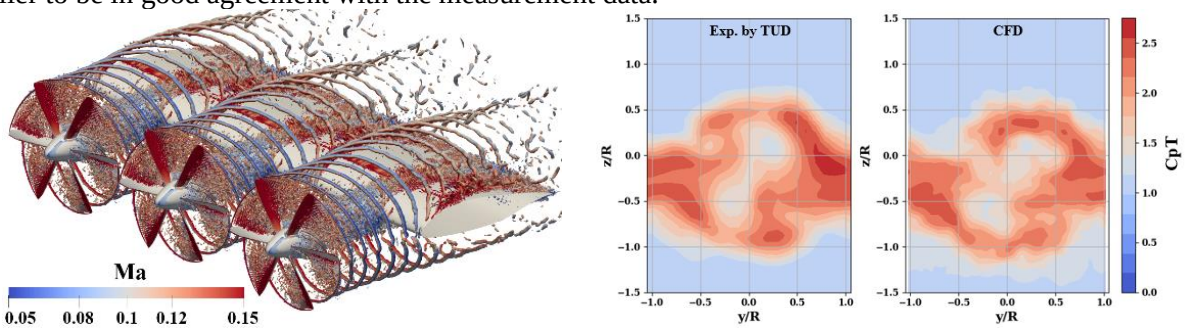

Figure 1: (a) The propeller wake and tip vortex structures denoted by Q-Criterion which is color coded by the local Mach number. (b) Total pressure coefficient (CpT) two chord length downstream of the wing.

In Fig 2(a), the instantaneous perturbed pressure field visualizes the sound waves radiated from the propeller blades and also scattered from the leading edge of the wing. In Fig 2(b), the acoustic spectra at the far-field observer 1 m away from the wing predicted by the Ffowcs-Williams and Hawkings method is shown. The FW-H predictions have good consistency with the wind tunnel measurement in the high-frequency broad-band range. Due to the small amount of simulated rotations of the propeller, the lower frequent tonal noise components are not well captured yet. In the workshop, the acoustic results will be updated and the directivity of far-field noise at different frequencies will be further analyzed.

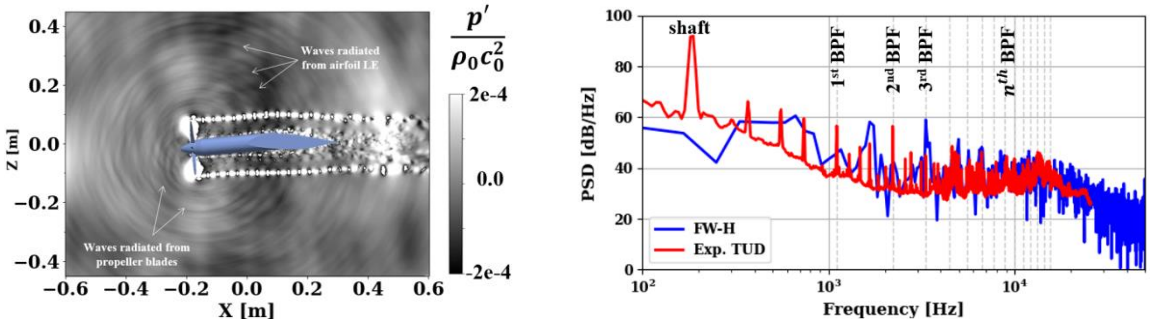

Figure 2: (a) Instantaneous perturbed pressure field *p*' around the propeller and wing. (b) Comparison of the predicted power spectral density (PSD) of the far-field noise with experimental data.

References

[1] Gohardani, A.S., Doulgeris, G. and Singh, R., 2011. Challenges of future aircraft propulsion: A review of distributed propulsion technology and its potential application for the all electric commercial aircraft. Progress in Aerospace Sciences, 47(5), pp.369-391.

[2] Agarwal, A. and Dowling, A.P., 2007. Low-frequency acoustic shielding by the silent aircraft air-frame. AIAA journal, 45(2), pp.358-365.

[3] Avallone, F., Casalino, D. and Ragni, D., 2018. Impingement of a propeller-slipstream on a leading edge with a flow-permeable insert: A computational aeroacoustic study. International Journal of Ae-roacoustics, 17(6-8), pp.687-711.

[4] Acevedo Giraldo, D., Roger, M. and Jacob, M.C., 2023. Experimental Study of the Aerodynamic Noise of a Pair of Pusher-Propellers Installed Over a Wing. In AIAA AVIATION 2023 Forum (p. 3359).

[5] Lintermann, A., Meinke, M. and Schröder, W., 2020. Zonal Flow Solver (ZFS): a highly efficient multi-physics simulation framework. International journal of computational fluid dynamics, 34(7-8), pp.458-485.

[6] Duivenvoorden, R., Suard, N., Sinnige, T. and Veldhuis, L.L., 2022. Experimental Investigation of Aerodynamic Interactions of a Wing with Deployed Fowler Flap under Influence of a Propeller Slipstream. In AIAA AVIATION 2022 Forum (p. 3216).